

1 **Integrating Zircon Trace Element Geochemistry and High-Precision**  
2 **U-Pb Zircon Geochronology to Resolve Timing and Petrogenesis of**  
3 **the late Ediacaran-Cambrian Wichita Igneous Province, Southern**  
4 **Oklahoma Aulacogen, USA**

5  
6 **Supplementary Material**

7  
8 **Corey J. Wall<sup>1\*</sup>, Richard E. Hanson<sup>2</sup>, Mark Schmitz<sup>1</sup>, Jonathan D. Price<sup>3</sup>,**  
9 **Nowell Donovan<sup>2</sup>, Joseph R. Boro<sup>4</sup>, Amy M. Eschberger<sup>5</sup>, Chelsea E. Toews<sup>6</sup>**

10  
11 *<sup>1</sup>Department of Geosciences, Boise State University, 1910 University Drive, Boise, ID, 83725,*  
12 *USA*

13 *<sup>2</sup>School of Geology, Energy and the Environment, Texas Christian University, Fort Worth, Texas*  
14 *78712, USA*

15 *<sup>3</sup>Kimbell School of Geosciences, Midwestern State University, Wichita Falls, Texas, 76308, USA*

16 *<sup>4</sup>School of the Environment, Washington State University, Pullman, Washington, 99164, USA*

17 *<sup>5</sup>Mining and Safety, Colorado Division of Reclamation, Denver, Colorado, 80203, USA*

18 *<sup>6</sup>Stewards, Conservation Legacy, Durango, Colorado, 81301, USA*

19

20

21

22 \*Corresponding author.

23 *email address: coreywall@boisestate.edu (C.J. Wall)*

24

25

## 26 Analytical Methods and Results

### 27 *Sample preparation*

28 An abundant population of relatively small (approximately 100-200  $\mu\text{m}$  in long  
29 dimension), equant to prismatic zircon crystals was separated from each hand sample by  
30 conventional density and magnetic methods. The entire zircon separate was placed in a muffle  
31 furnace at 900°C for 60 hours in quartz beakers to anneal minor radiation damage; annealing  
32 enhances cathodoluminescence (CL) emission (Nasdala et al., 2002), promotes more  
33 reproducible interelement fractionation during laser ablation inductively coupled plasma mass  
34 spectrometry (LA-ICPMS) (Allen and Campbell, 2012), and prepares the crystals for subsequent  
35 chemical abrasion (Mattinson, 2005). Following annealing, individual grains were hand-picked  
36 and mounted, polished and imaged by CL on a scanning electron microscope. From these  
37 compiled images, the locations of spot analyses for LA-ICP-MS were selected.

38

### 39 *LA-ICPMS analysis*

40 LA-ICPMS analysis utilized an X-Series II quadrupole ICPMS and New Wave Research  
41 UP-213 Nd:YAG UV (213 nm) laser ablation system. In-house analytical protocols, standard  
42 materials, and data reduction software were used for acquisition and calibration of U-Pb dates  
43 and a suite of high field strength elements (HFSE) and rare earth elements (REE). Zircon was  
44 ablated with a laser raster 15  $\mu\text{m}$  wide using fluence and pulse rates of  $\sim 5 \text{ J/cm}^2$  and 20 Hz,  
45 during a 45 second analysis (15 sec gas blank, 30 sec ablation) that excavated a line  $\sim 5 \mu\text{m}$  deep.  
46 Ablated material was carried by a 1.15 L/min He gas stream to the nebulizer flow of the plasma.  
47 Quadrupole dwell times were 5 ms for Si and Zr, 200 ms for  $^{49}\text{Ti}$  and  $^{207}\text{Pb}$ , 80 ms for  $^{206}\text{Pb}$ , 40  
48 ms for  $^{202}\text{Hg}$ ,  $^{204}\text{Pb}$ ,  $^{208}\text{Pb}$ ,  $^{232}\text{Th}$ , and  $^{238}\text{U}$  and 10 ms for all other HFSE and REE; total sweep  
49 duration is 950 ms. Background count rates for each analyte were obtained prior to each line  
50 analysis and subtracted from the raw count rate for each analyte. For concentration calculations,  
51 background-subtracted count rates for each analyte were internally normalized to  $^{29}\text{Si}$  and  
52 calibrated with respect to NIST SRM-610 and -612 glasses as the primary standards. Ablation  
53 pits that appeared to have intersected glass or mineral inclusions were identified based on Ti and  
54 P signal excursions, and data from those analyses were generally discarded. U-Pb dates from  
55 these analyses were considered valid if the U-Pb ratios appeared to have been unaffected by the  
56 inclusions. Signals at mass 204 were normally indistinguishable from zero following subtraction

57 of mercury backgrounds measured during the gas blank ( $<100$  cps  $^{202}\text{Hg}$ ), and thus dates are  
58 reported without common Pb correction. Rare analyses that appeared contaminated by common  
59 Pb were rejected based on mass 204 greater than baseline. Additionally, elements sensitive to  
60 micro-inclusions of apatite, monazite, rutile, oxides, and melt inclusions (e.g., P, Ti, LREE) were  
61 monitored if there were excursions in these elements, these analyses were rejected and not  
62 included for interpretations in this study. Temperature was calculated from the Ti-in-zircon  
63 thermometer (Watson et al., 2006). Because there are no constraints on the activity of  $\text{TiO}_2$  in the  
64 source rocks, an average value in crustal rocks of 0.8 was used and an activity of  $\text{SiO}_2$  of 1.0 was  
65 used based on the presence of quartz in all samples (Hayden and Watson, 2007).

66 For U-Pb and  $^{207}\text{Pb}/^{206}\text{Pb}$  dates, instrumental fractionation of the background-subtracted  
67 ratios was corrected and dates were calibrated with respect to interspersed measurements of  
68 zircon standards and reference materials. The primary standard Plešovice zircon (Sláma et al.,  
69 2008) was used to monitor time-dependent instrumental fractionation based on two analyses for  
70 every 10 analyses of unknown zircon. A polynomial fit to the primary standard analyses versus  
71 time yields each sample-specific fractionation factor. A secondary bias correction was  
72 subsequently applied to unknowns on the basis of the residual age bias as a function of  
73 radiogenic Pb count rate in standard materials, including Seiland, Zirconia, and Plesovice zircon,  
74 or similar materials of known age and variable Pb content. A polynomial fit to the secondary  
75 standard analyses with Pb count rate yields each sample-specific bias correction. Radiogenic  
76 isotope ratio and age error propagation for all analyses includes uncertainty contributions from  
77 counting statistics and background subtraction. Because the detrital zircon analyses are  
78 interpreted individually, uncertainties from the standard calibrations are propagated into the  
79 errors on each date. These uncertainties are the local standard deviations of the polynomial fits to  
80 the interspersed primary standard measurements versus time for the time-dependent, relatively  
81 larger U/Pb fractionation factor, and the standard errors of the means of the consistently time-  
82 invariant and smaller  $^{207}\text{Pb}/^{206}\text{Pb}$  fractionation factor. These uncertainties are  $\sim 2\%$  ( $2\sigma$ ) for  
83  $^{206}\text{Pb}/^{238}\text{U}$  and  $\sim 1\%$  ( $2\sigma$ ) for  $^{207}\text{Pb}/^{206}\text{Pb}$ . Additional details of methodology and reproducibility  
84 are reported in Rivera et al. (2013).

85

86 ***ID-TIMS analysis***

87 U-Pb geochronology methods for isotope dilution thermal ionization mass spectrometry  
88 follow those previously published by Davydov et al. (2010) and Schmitz and Davydov (2012).  
89 All analyses were undertaken on crystals previously mounted, polished and imaged by  
90 cathodoluminescence (CL), and analyzed by LA-ICPMS. Zircon crystals were subjected to a  
91 modified version of the chemical abrasion method of Mattinson (2005), whereby single crystal  
92 fragments plucked from grain mounts were individually abraded in a single step with  
93 concentrated HF at 190°C for 12 hours. Zircon fragments were dissolved in Parr bombs at 220  
94 °C for 48 h. Dissolved zircon solutions were subsequently dried down, redissolved in 100 µl 6 N  
95 HCl and converted to chlorides in Parr bombs at 180 °C for 12 h, after which solutions were  
96 dried again and brought up in 50 µl 3 N HCl. U and Pb were isolated by anion exchange column  
97 chromatography using 50 µl columns and AG-1 X8 resin [200–400 mesh, chloride form  
98 (Eichrom); Krogh, 1973].

99 The U-Pb aliquot was loaded in a silica gel emitter (Gerstenberger & Haase, 1997) to an  
100 outgassed, zone-refined Re filament. Isotopic determinations were performed using an IsotopX  
101 PhoeniX-62 TIMS. A correction for mass-dependent Pb fractionation was applied based on  
102 repeated measurements of NBS 982 (Catanzaro et al., 1968) Pb on both the Daly ion counter  
103 [ $0.16 \pm 0.03$  %]  $\text{amu}^{-1}$ ; 1s] and the Faraday cups [ $0.10 \times (1 \pm 0.02$  %]  $\text{amu}^{-1}$ ; 1s]. Uranium was  
104 run as an oxide ( $\text{UO}_2$ ) and measured in static mode on Faraday detectors equipped with  $10^{12}$  Ω  
105 resistors. The U mass fractionation for the same analyses was calculated using the  $^{233}\text{U}/^{235}\text{U}$  ratio  
106 of the double spike solution ( $0.99506$  %  $\pm 0.01$  %, 1s).

107 U-Pb dates and uncertainties for each analysis were calculated using the algorithms of  
108 Schmitz and Schoene (2007), the U decay constants of Jaffey et al. (1971), and a value of  
109  $^{238}\text{U}/^{235}\text{U} = 137.88$ . Uranium oxide measurements were corrected for isobaric interferences using  
110 an  $^{18}\text{O}/^{16}\text{O}$  value of 0.00206. Uncertainties are based upon non-systematic analytical errors,  
111 including counting statistics, instrumental fractionation, tracer subtraction, and blank subtraction.  
112 All non-radiogenic Pb was attributed to laboratory blank with a mean isotopic composition  
113 determined by total procedural blank measurements. These error estimates should be considered  
114 when comparing our  $^{206}\text{Pb}/^{238}\text{U}$  dates with those from other laboratories that used tracer solutions  
115 calibrated against the EARTHTIME gravimetric standards. When comparing our dates with  
116 those derived from other decay schemes (e.g.,  $^{40}\text{Ar}/^{39}\text{Ar}$ ,  $^{187}\text{Re}$ - $^{187}\text{Os}$ ), the uncertainties in tracer  
117 calibration (0.05%; Condon et al., 2015; McLean et al., 2015) and U decay constants (0.108%;

118 Jaffey et al., 1971) should be added to the internal error in quadrature. Quoted errors for  
119 calculated weighted means are thus of the form  $\pm X(Y)[Z]$ , where X is solely analytical  
120 uncertainty, Y is the combined analytical and tracer uncertainty, and Z is the combined  
121 analytical, tracer and  $^{238}\text{U}$  decay constant uncertainty.

122 **G8 (Anorthosite from Glen Mountains Layered Complex):** CL-imaging of the 50  
123 largest zircon crystals from this sample revealed a homogenous population of moderately  
124 luminescent, oscillatory to sector zoned crystals. Nine grains were selected for CA-TIMS  
125 analysis on the basis of the uniform, predominant CL pattern. Chemical abrasion in concentrated  
126 HF at 190°C for 12 hours resulted in moderate dissolution of the zircon crystals. All eight  
127 analyses are concordant and equivalent, with a weighted mean  $^{206}\text{Pb}/^{238}\text{U}$  date of  $532.49 \pm$   
128  $0.12(0.28)[0.62]$  Ma (MSWD = 0.93), which is interpreted as dating the crystallization of this  
129 anorthosite.

130 **AE-389 (Rhyolite from the Arbuckle Mountains):** CL-imaging of the 100 largest  
131 zircon crystals from this sample revealed a homogenous population of moderately luminescent,  
132 oscillatory to sector zoned crystals. A lesser number of crystals have irregularly shaped,  
133 relatively non-luminescent cores overgrown by aforementioned luminescent, oscillatory rims.  
134 There are also a few zircon crystals that are poorly luminescent but are oscillatory zoned and are  
135 considered to be xenocrysts. Eight grains were selected for CA-TIMS analysis on the basis of the  
136 uniform, predominant CL pattern. Chemical abrasion in concentrated HF at 190°C for 12 hours  
137 resulted in moderate dissolution of the zircon crystals. All eight analyses are concordant and  
138 equivalent, with a weighted mean  $^{206}\text{Pb}/^{238}\text{U}$  date of  $539.20 \pm 0.15(0.30)[0.64]$  Ma (MSWD =  
139 0.54), which is interpreted as dating the eruption age of this rhyolite.

140 **JP-22 (Rhyolite flow from base of volcanic succession at Bally Mountain):**

141 CL-imaging of the 100 largest zircon crystals from this sample revealed a homogenous  
142 population of moderately luminescent, oscillatory to sector zoned crystals. A lesser number of  
143 crystals have irregularly shaped, relatively non-luminescent cores overgrown by aforementioned  
144 luminescent, oscillatory rims. There are also a few zircon crystals that are poorly luminescent but  
145 are oscillatory zoned and are considered to be xenocrysts. Eight grains were selected for CA-  
146 TIMS analysis on the basis of the uniform, predominant CL pattern. Chemical abrasion in  
147 concentrated HF at 190°C for 12 hours resulted in moderate dissolution of the zircon crystals.  
148 All eight analyses are concordant and equivalent, with a weighted mean  $^{206}\text{Pb}/^{238}\text{U}$  date of

149 530.98 ± 0.14 Ma(0.29)[0.62] Ma (MSWD = 0.94), which is interpreted as dating the eruption  
150 age of this rhyolite.

151 **JP-120 (Rhyolite flow from top of volcanic succession at Bally Mountain):**

152 CL-imaging of the 100 largest zircon crystals from this sample revealed a homogenous  
153 population of moderately luminescent, oscillatory to sector zoned crystals. A lesser number of  
154 crystals have irregularly shaped, relatively non-luminescent cores overgrown by aforementioned  
155 luminescent, oscillatory rims. There are also a few zircon crystals that are poorly luminescent but  
156 are oscillatory zoned and are considered to be xenocrysts. Thirteen grains were selected for CA-  
157 TIMS analysis on the basis of the uniform, predominant CL pattern. Chemical abrasion in  
158 concentrated HF at 190°C for 12 hours resulted in moderate dissolution of the zircon crystals.  
159 All thirteen analyses are concordant and equivalent, with a weighted mean  $^{206}\text{Pb}/^{238}\text{U}$  date of  
160 530.70 ± 0.12 Ma(0.28)[0.62] Ma (MSWD = 0.81), which is interpreted as dating the eruption  
161 age of this rhyolite.

162 **WP16-2 (Mt. Scott Granite):**

163 CL-imaging of the 100 largest zircon crystals from this sample revealed a homogenous  
164 population of moderately luminescent, oscillatory to sector zoned crystals. A lesser number of  
165 crystals have irregularly shaped, relatively non-luminescent cores overgrown by aforementioned  
166 luminescent, oscillatory rims. There are also a few zircon crystals that are poorly luminescent but  
167 are oscillatory zoned and are considered to be xenocrysts. Eight grains were selected for CA-  
168 TIMS analysis on the basis of the uniform, predominant CL pattern. Chemical abrasion in  
169 concentrated HF at 190°C for 12 hours resulted in moderate dissolution of the zircon crystals.  
170 All eight analyses are concordant and equivalent, with a weighted mean  $^{206}\text{Pb}/^{238}\text{U}$  date of  
171 530.45 ± 0.14 Ma(0.29)[0.62] Ma (MSWD = 0.69), which is interpreted as dating the  
172 crystallization of this granite.

173 **WP18-1 (Cache Granite):**

174 CL-imaging of the 55 largest zircon crystals from this sample revealed a homogenous  
175 population of moderately luminescent, oscillatory to sector zoned crystals. A lesser number of  
176 crystals have irregularly shaped, relatively non-luminescent cores overgrown by aforementioned  
177 luminescent, oscillatory rims. There are also a few zircon crystals that are poorly luminescent but  
178 are oscillatory zoned and are considered to be xenocrysts. Seven grains were selected for CA-  
179 TIMS analysis on the basis of the uniform, predominant CL pattern. Chemical abrasion in

180 concentrated HF at 190°C for 12 hours resulted in moderate dissolution of the zircon crystals.  
181 All seven analyses are concordant and equivalent, with a weighted mean  $^{206}\text{Pb}/^{238}\text{U}$  date of  
182  $530.61 \pm 0.13 \text{ Ma}(0.29)[0.62] \text{ Ma}$  (MSWD = 0.12), which is interpreted as dating the  
183 crystallization of this granite.

#### 184 **JPQ-71797 (Quanah Granite):**

185 CL-imaging of the 60 largest zircon crystals from this sample revealed a homogenous  
186 population of moderately luminescent, oscillatory to sector zoned crystals. A lesser number of  
187 crystals have irregularly shaped, relatively non-luminescent cores overgrown by aforementioned  
188 luminescent, oscillatory rims. There are also a few zircon crystals that are poorly luminescent but  
189 are oscillatory zoned and are considered to be xenocrysts. Eight grains were selected for CA-  
190 TIMS analysis on the basis of the uniform, predominant CL pattern. Chemical abrasion in  
191 concentrated HF at 190°C for 12 hours resulted in moderate dissolution of the zircon crystals.  
192 Six of the eight analyses are concordant and equivalent, with a weighted mean  $^{206}\text{Pb}/^{238}\text{U}$  date of  
193  $530.23 \pm 0.14 \text{ Ma}(0.29)[0.62] \text{ Ma}$  (MSWD = 0.12), which is interpreted as dating the  
194 crystallization of this granite.

195

#### 196 **REFERENCES**

197

198 Allen, C.M., Campbell, I.H., 2012. Identification and elimination of a matrix-induced systematic  
199 error in LA-ICP-MS  $^{206}\text{Pb}/^{238}\text{U}$  dating of zircon: *Chemical Geology* 332-333, 157–165.  
200 doi:10.1016/j.chemgeo.2012.09.038

201 Catanzaro, E.J., Murphy, T.J., Shields, W.R., Garner, E.L., 1968, Absolute isotopic abundance of  
202 common, equal-atom, and radiogenic lead isotopic standards: *Journal of Research of the*  
203 *NAtiional Bureau of Standards – A. Physics and Chemistry*, v. 72A, n. 3, p. 261-267.

204 Condon, D.J., Schoene, B., McLean, N.M., Bowring, S.A., Parrish, R.R., 2015. Metrology and  
205 traceability of U-Pb isotope dilution geochronology (EARTHTIME Tracer Calibration  
206 Part I): *Geochimica et Cosmochimica Acta* 164, 464–480. doi:10.1016/j.gca.2015.05.026

207 Davydov, V. I., Crowley, J. L., Schmitz, M. D., and Poletaev, V. I., 2010, High-precision U-Pb  
208 zircon age calibration of the global Carboniferous time scale and Milankovitch-band  
209 cyclicity in the Donets Basin, eastern Ukraine: *Geochemistry, Geophysics, Geosystems*,  
210 10.1029/2009GC002736.

211 Gerstenberger, H., and Haase, G.A., 1997, Highly effective emitter substance for mass  
212 spectrometric Pb isotope ratio determinations: *Chemical Geology*, v. 136, p. 309-312.

213 Hayden, L. A., and Watson, E. B., 2007, Rutile saturation in hydrous siliceous melts and its  
214 bearing on Ti-thermometry of quartz and zircon: *Earth and Planetary Science Letters*, v.  
215 258, p. 561-568.

216 Jaffey, A.H., Flynn, K.F., Glendenin, L.E., Bentley, W.C., and Essling, A.M., 1971, Precision  
217 measurements of half-lives and specific activities of  $^{235}\text{U}$  and  $^{238}\text{U}$ : *Physical Review C*,  
218 4:1889-1906.

219 Krogh, T.E., 1973, A low contamination method for hydrothermal decomposition of zircon and  
220 extraction of U and Pb for isotopic age determinations: *Geochimica et Cosmochimica*  
221 *Acta*, v. 37, p. 485-494.

222 Mattinson, J.M., 2005, Zircon U-Pb chemical abrasion ("CA-TIMS") method: combined  
223 annealing and multi-step partial dissolution analysis for improved precision and accuracy  
224 of zircon ages: *Chemical Geology* 220:47-66.

225 McLean, N.M., Condon, D.J., Schoene, B., Bowring, S.A., 2015. Evaluating uncertainties in the  
226 calibration of isotopic reference materials and multi-element isotopic tracers  
227 (EARTHTIME Tracer Calibration Part II): *Geochimica et Cosmochimica Acta* 164, 481–  
228 501. doi:10.1016/j.gca.2015.02.040.

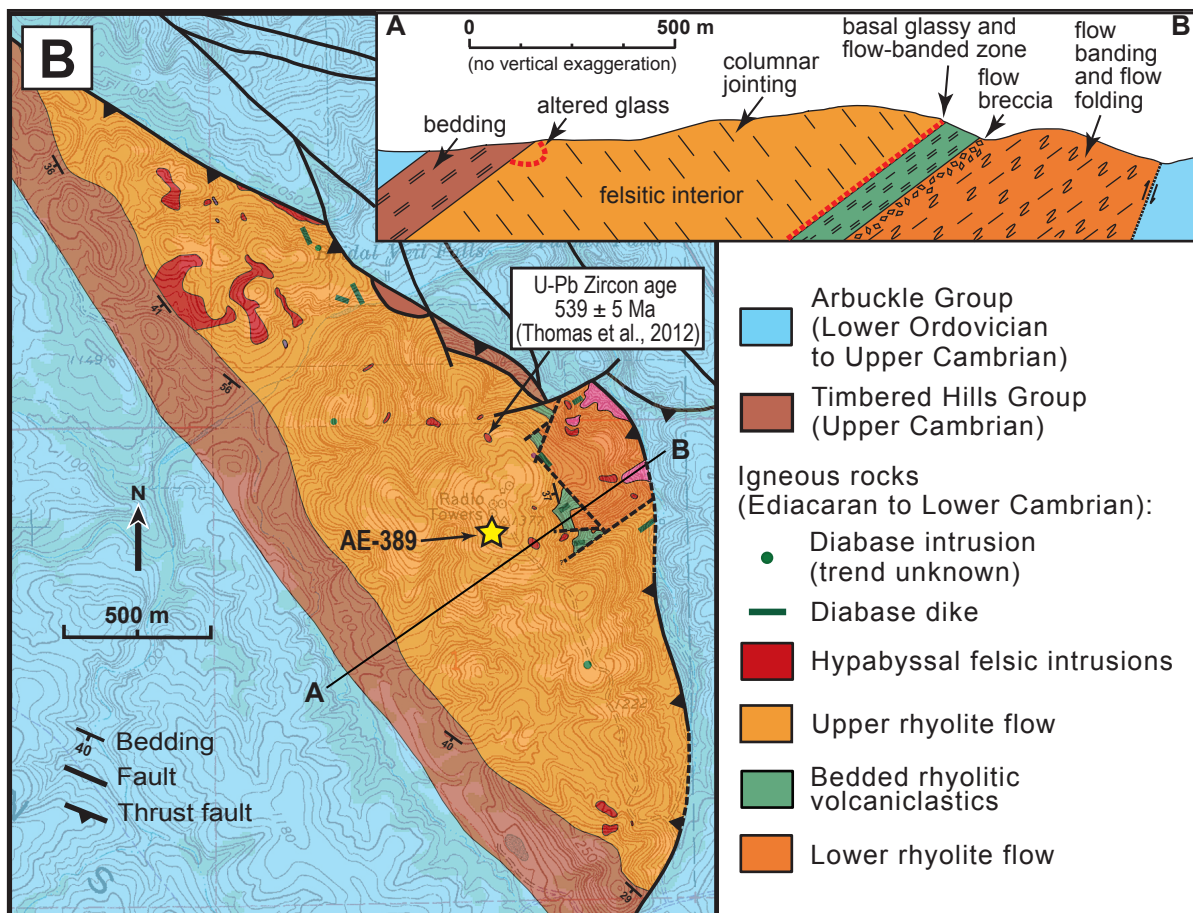
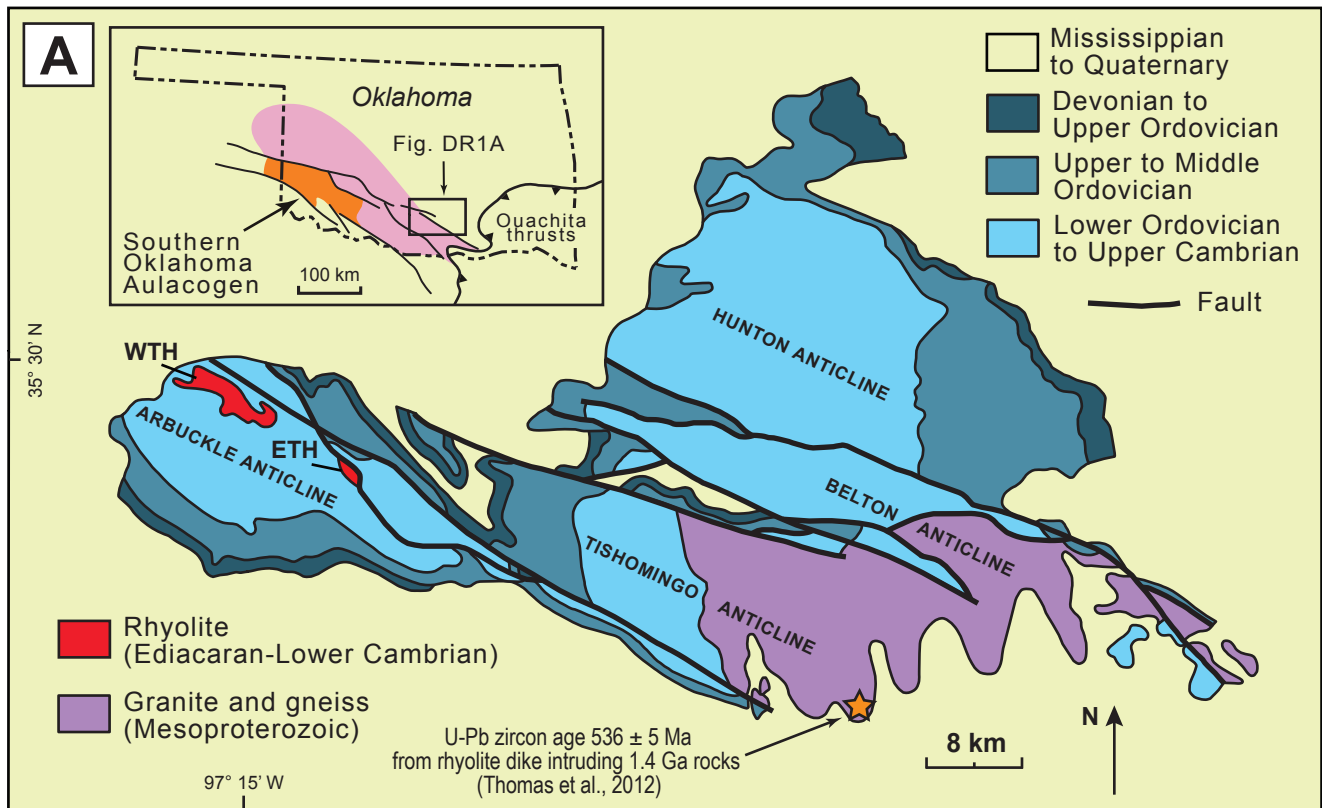
229 Nasdala, L., Lengauer, C.L., Hanchar, J.M., Kronz, A., Wirth, R., Blanc, P., Kennedy, A.K.,  
230 Seydoux-Guillaume, A.M., 2002. Annealing radiation damage and the recovery of  
231 cathodoluminescence: *Chemical Geology* 191, 121–140.

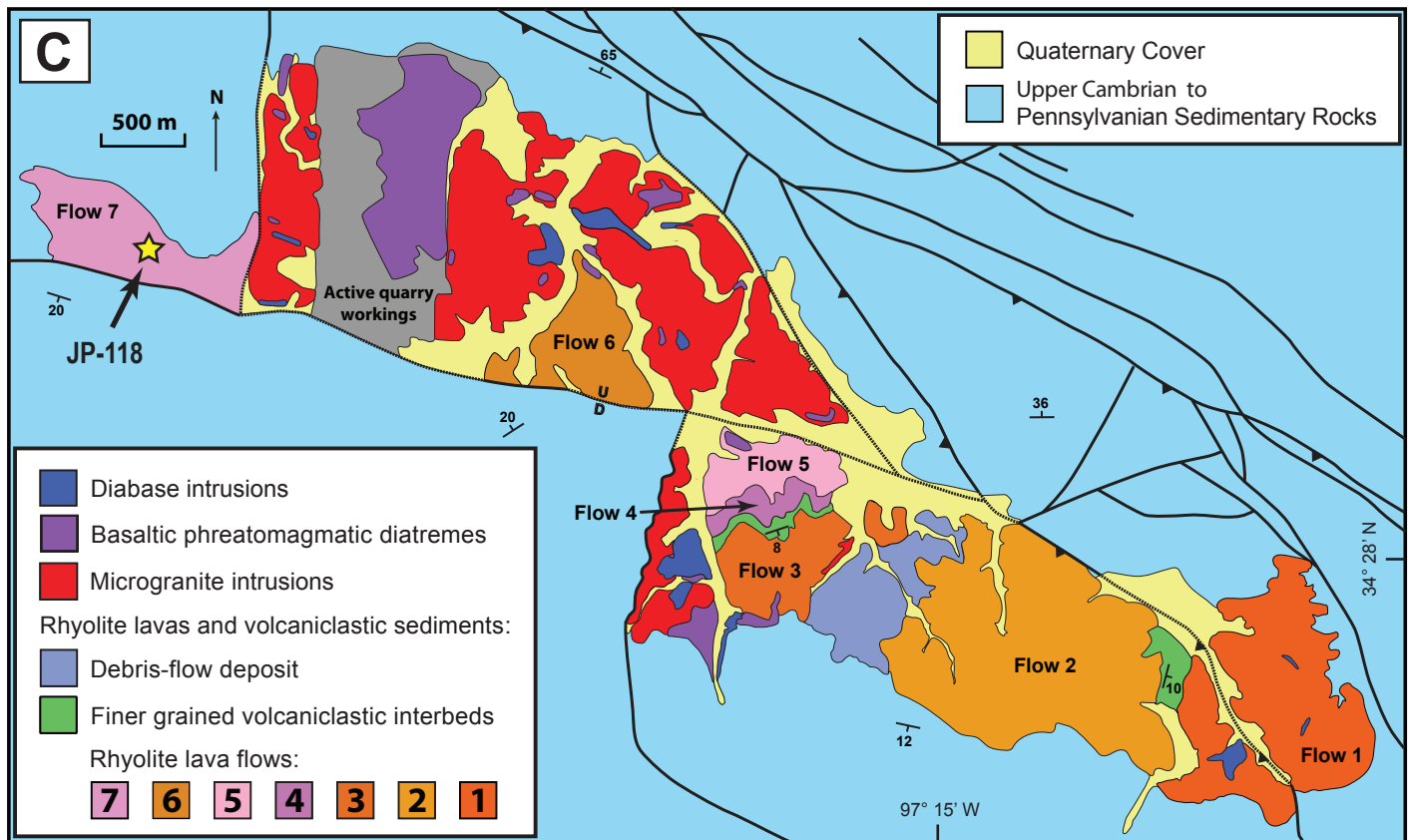
232 Rivera, T.A., Storey, M., Schmitz, M.D., Crowley, J.L., 2013. Age intercalibration of  $^{40}\text{Ar}/^{39}\text{Ar}$   
233 sanidine and chemically distinct U/Pb zircon populations from the Alder Creek Rhyolite  
234 Quaternary geochronology standard: *Chemical Geology* 345, 87–98.

235 Schmitz, M.D., Schoene, B., 2007, Derivation of isotope ratios, errors and error correlations for  
236 U-Pb geochronology using  $^{205}\text{Pb}$ - $^{235}\text{U}$ -( $^{233}\text{U}$ )-spiked isotope dilution thermal ionization  
237 mass spectrometric data: *Geochemistry, Geophysics, Geosystems* 8, Q08006,  
238 doi:10.1029/2006GC00149

239 Schmitz, M.D., Davydov, V.I., 2012, Quantitative radiometric and biostratigraphic calibration of  
240 the global Pennsylvanian – Early Permian time scale: *Geological Society of America*  
241 *Bulletin*, 124:549-577.

- 242 Sláma, J., Košler, J., Condon, D., and Crowley, J., 2008, Plešovice zircon – A new natural  
243 reference material for U–Pb and Hf isotopic microanalysis: *Chemical Geology*, v. 249, p.  
244 1-35.
- 245 Watson, E.B., Wark, D.A., Thomas, J.B. 2006. Crystallization thermometers for zircon and rutile:  
246 *Contributions to Mineralogy and Petrology*, 151: 413-433.

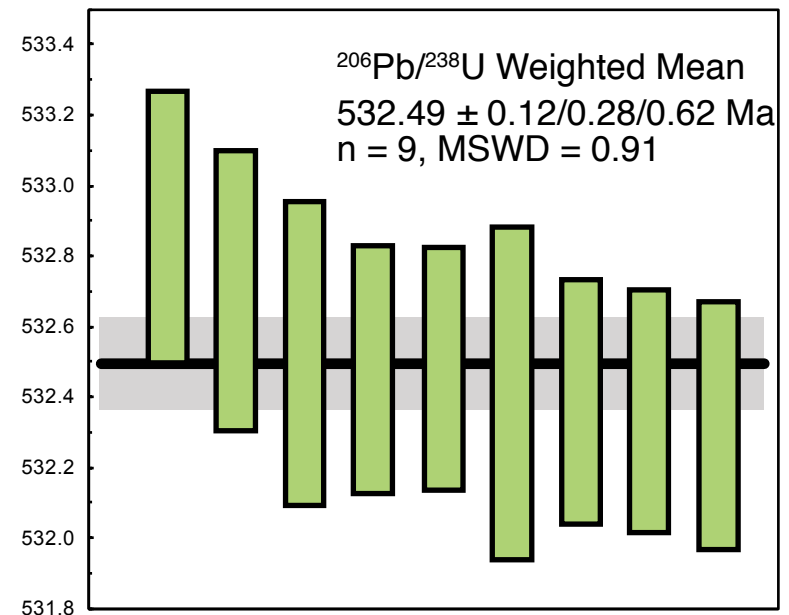
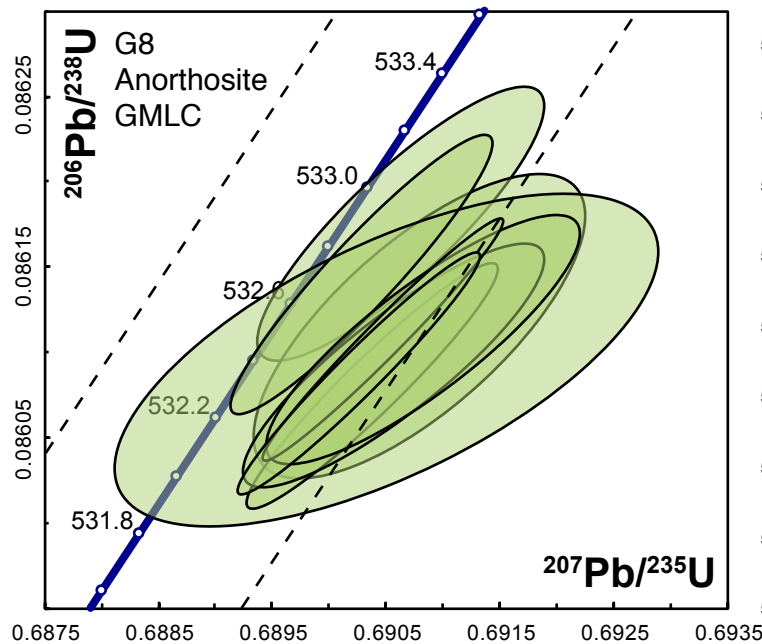
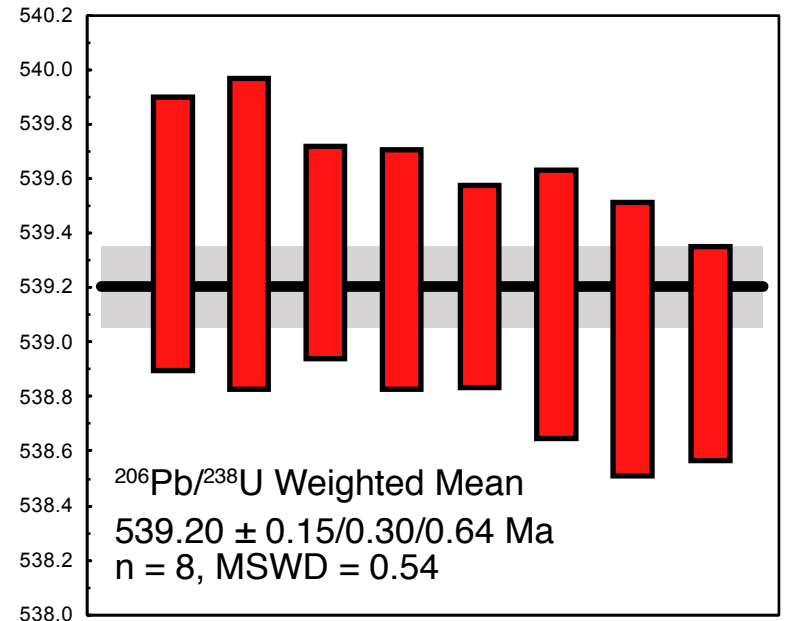
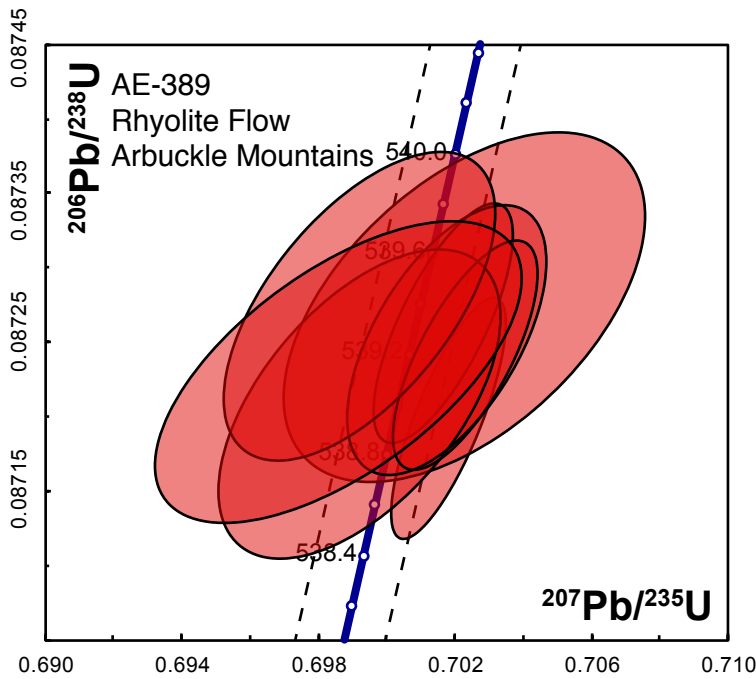
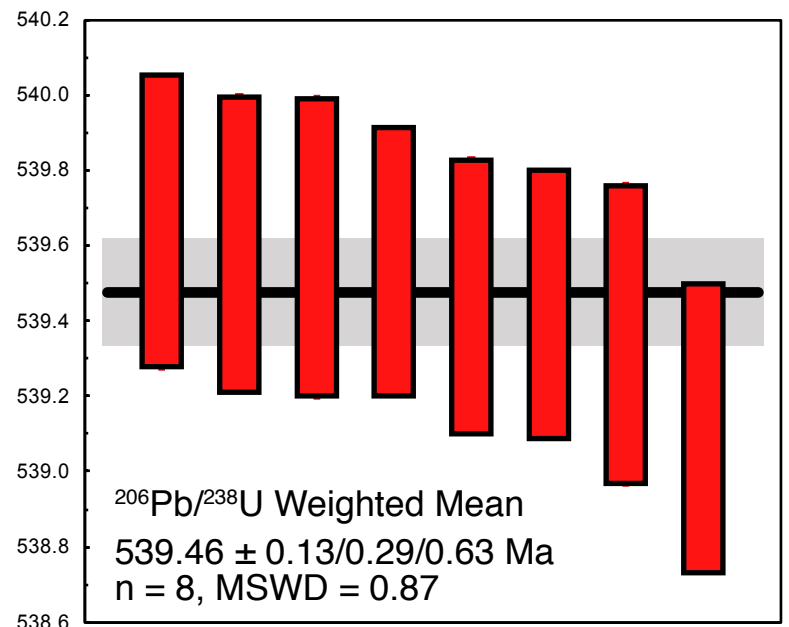
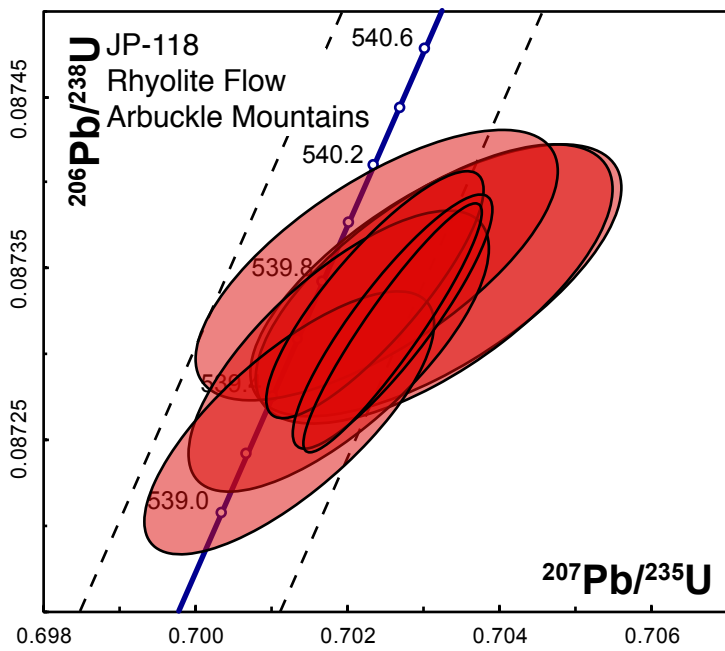


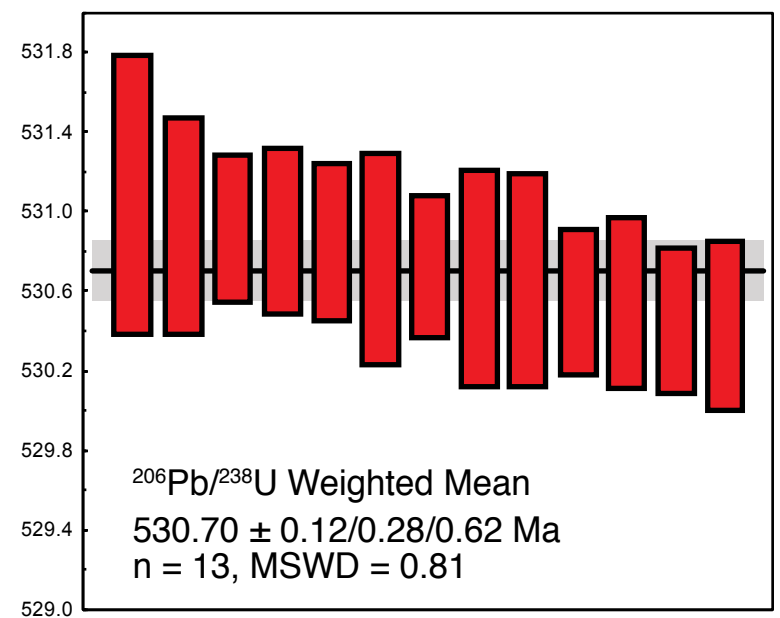
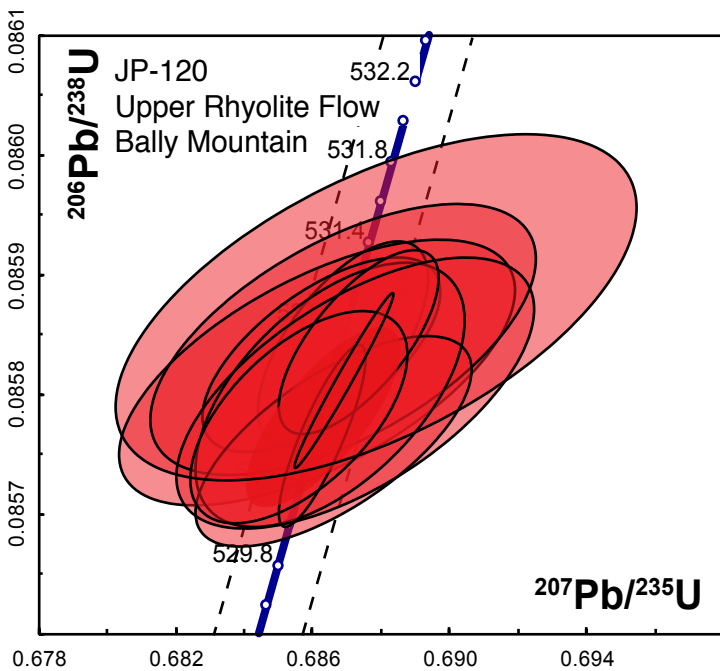
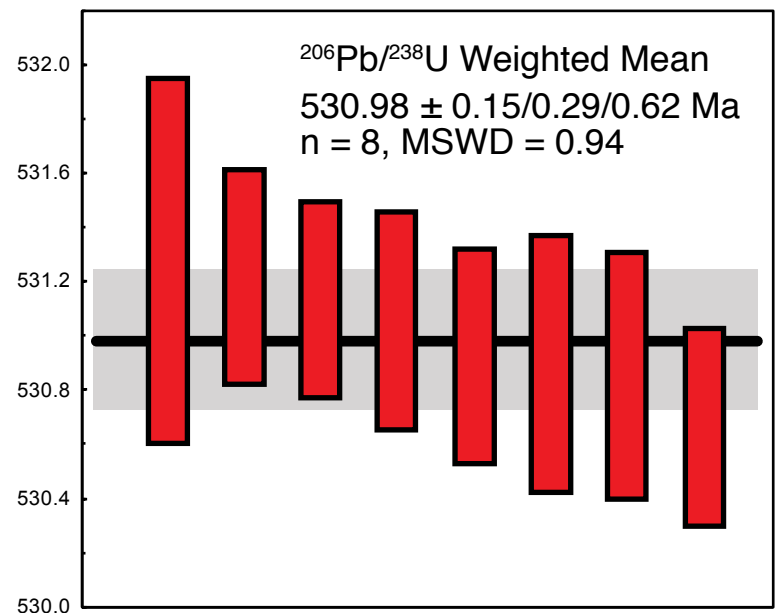
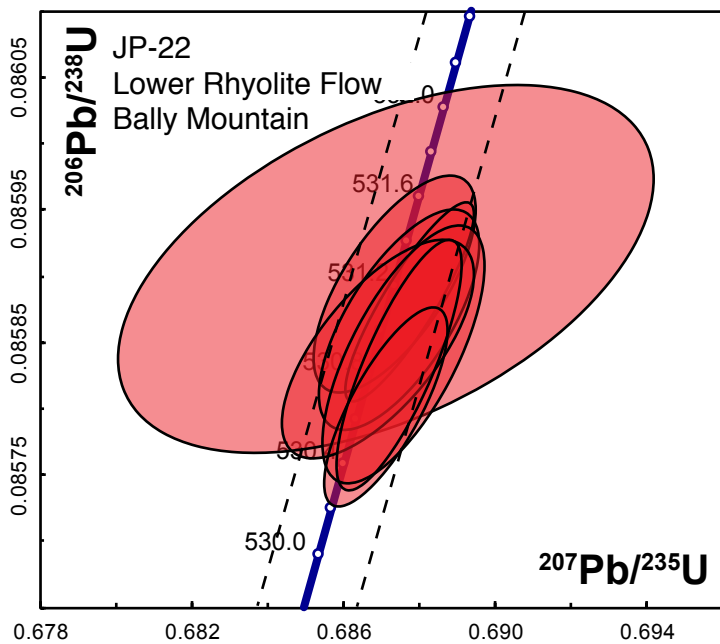
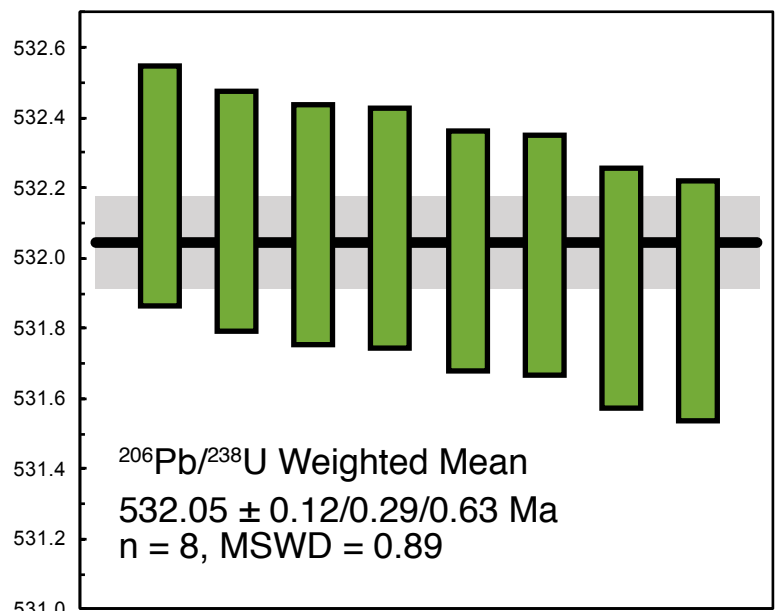
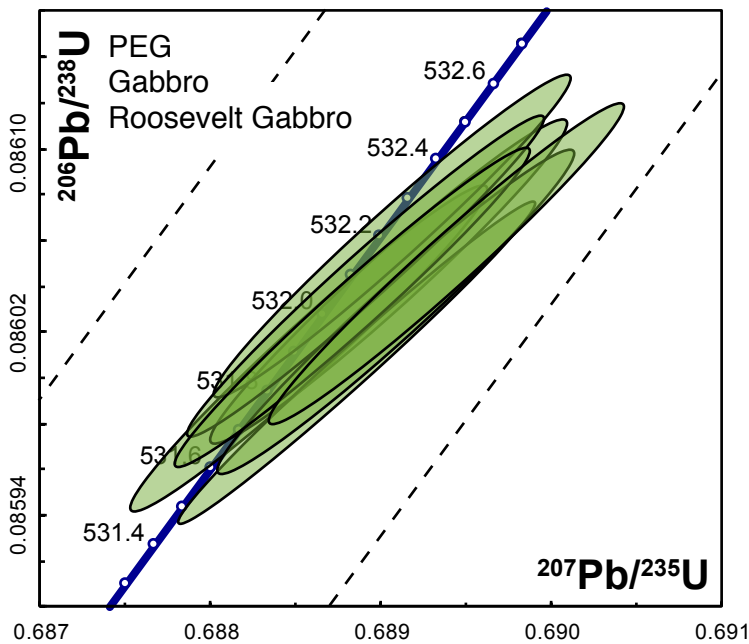


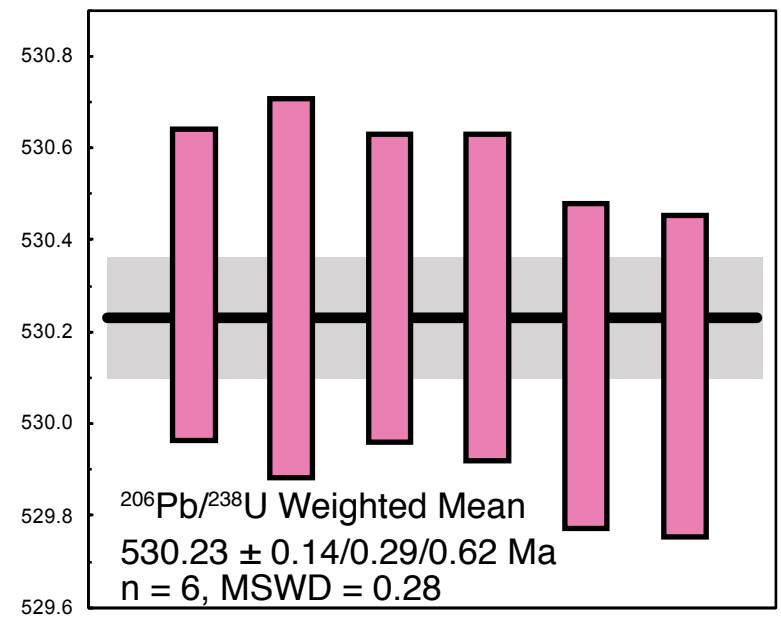
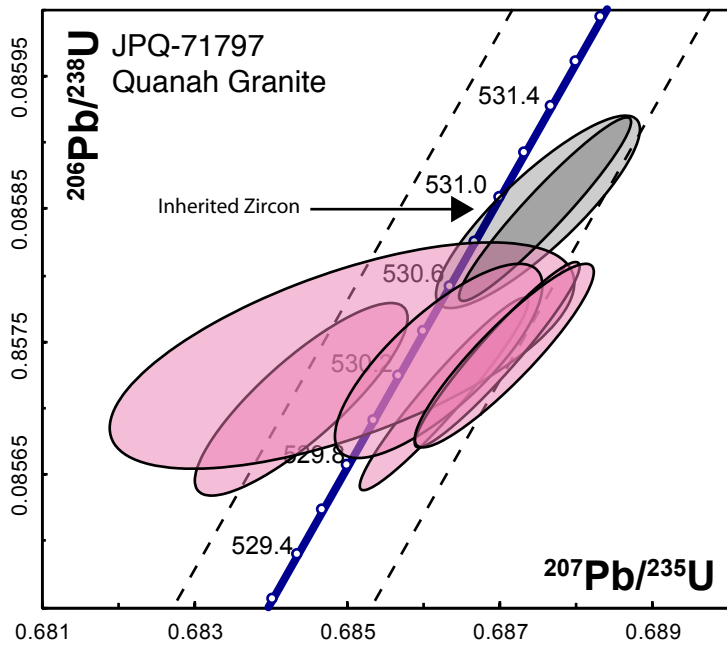
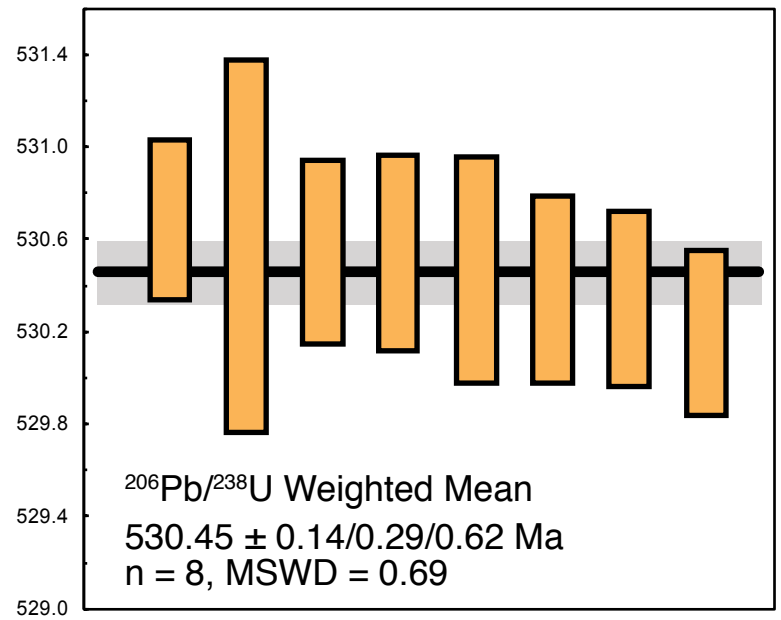
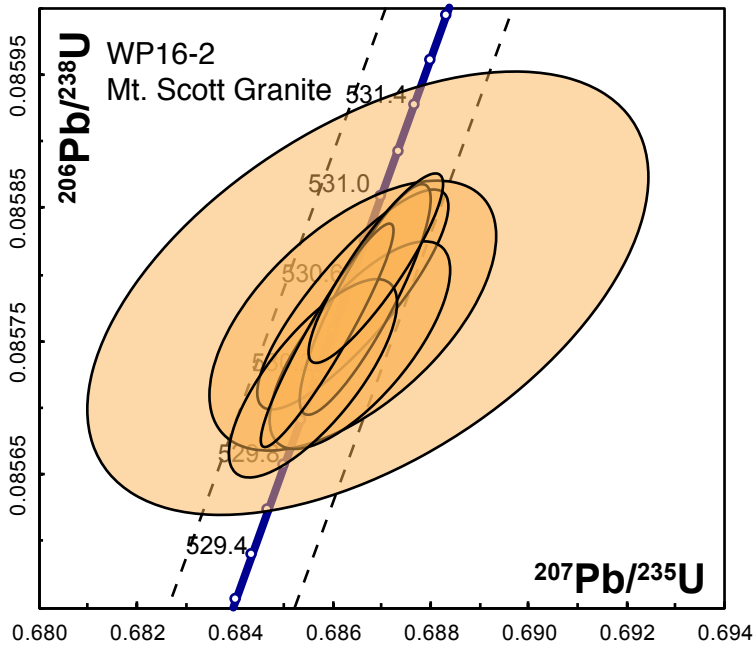
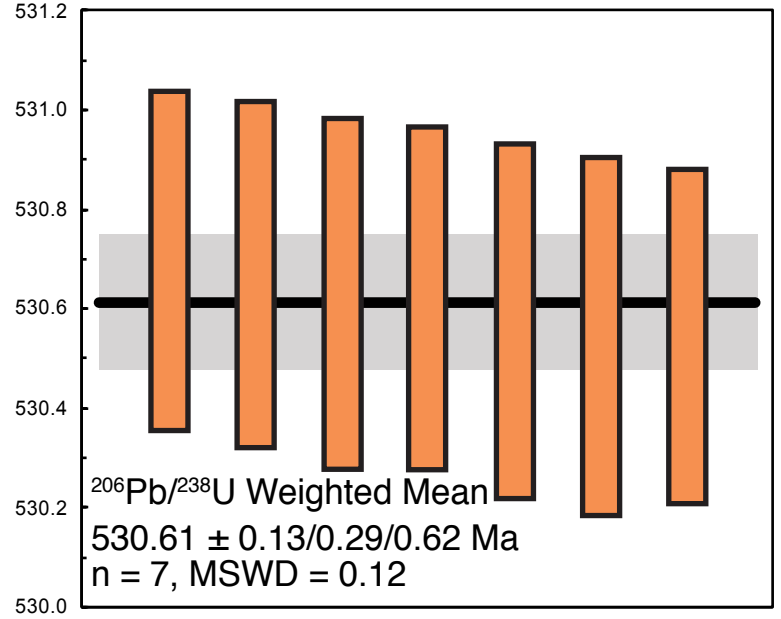
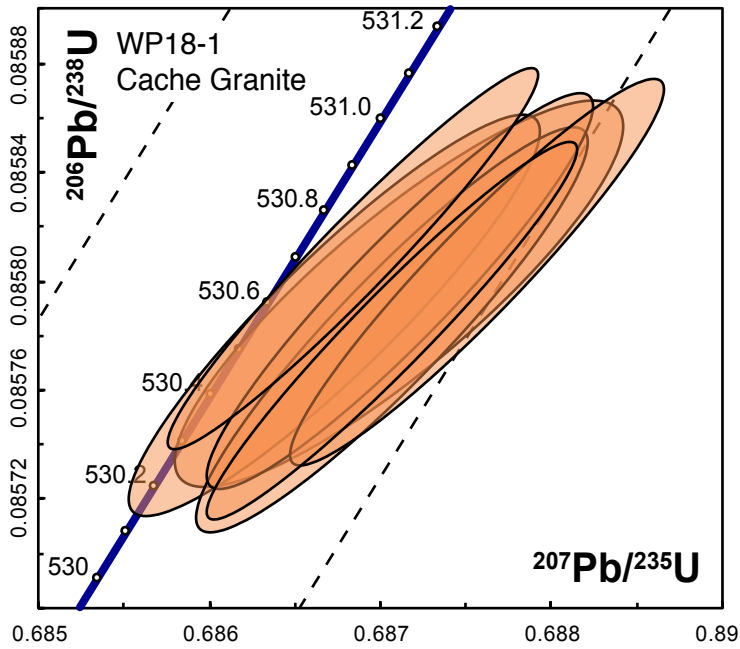
**Fig. DR1:** Geological setting of Arbuckle rhyolite samples. (A) Geological map of Arbuckle Mountains, modified from Ham (1973). WTH = West Timbered Hills, ETH = East Timbered Hills. Location of map is shown in inset. (B) Geological map and cross-section of igneous exposures in East Timbered Hills, modified from Eschberger et al. (2014). Location of dated rhyolite sample AE389 is indicated, along with location of hypabyssal felsic intrusion dated by Thomas et al. (2012). Faults are from Johnson (1990). (C) Geological map of igneous exposures in West Timbered Hills, modified from Boro (2015) and Toews (2015). Location of dated rhyolite sample JP-118 is indicated. Faults are generally taken from Johnson (1990).

#### References:

- Boro, J.R., 2015, Volcanic lithofacies and geochemistry of Cambrian rift-related rhyolites in the West Timbered Hills, Arbuckle Mountains, southern Oklahoma [M.S. thesis]: Fort Worth, Texas, Texas Christian University, 101 p.
- Eschberger, A.M., Hanson, R.E., and Puckett, R.E. Jr., 2014, Carlton Rhyolite Group and diabase intrusions in the East Timbered Hills, Arbuckle Mountains, in Suneson, N., ed., Igneous and Tectonic History of the Southern Oklahoma Aulacogen: Oklahoma Geological Survey Guidebook 38, p. 143–186.
- Ham, W.E., 1973, Regional geology of the Arbuckle Mountains, Oklahoma: Oklahoma Geological Survey Special Publication 73-3, 61 p.
- Johnson, K.S., 1990, Geologic map and sections of the Arbuckle Mountains, Oklahoma: Oklahoma Geological Survey Circular 91, Plate 1 of 2.
- Thomas, W.A., Tucker, R.D., Astini, R.A., and Denison, R.E., 2012, Ages of pre-rift basement and synrift rocks along the conjugate rift and transform margins of the Argentine Precordillera and Laurentia: *Geosphere*, v. 8, no. 6, p. 1–18. <https://doi.org/10.1130/GES00800.1>
- Toews, C.E., 2015, Cambrian phreatomagmatic igneous breccia and associated bimodal hypabyssal intrusion3 in the West Timbered Hills, Arbuckle Mountains, southern Oklahoma [M.S. thesis]: Fort Worth, Texas, Texas Christian University, 103 p.







Quoted errors for calculated  $^{206}\text{Pb}/^{238}\text{U}$  weighted means are of the form  $\pm X/Y/Z$ , where X is solely analytical uncertainty, Y is the combined analytical and tracer uncertainty, and Z is the combined analytical, tracer and  $^{238}\text{U}$  decay constant uncertainty. Each ellipse indicates the analysis of a single zircon grain. Dashed lines show the error bounds of the concordia curve due to the uncertainty in the decay constants of U. MSWD refers to the mean square of the weighted deviates. Horizontal black in the the weighted mean panel indicates the weighted mean date and the grey band reflects the internal uncertainty. Colors of the ellipses and individual  $^{206}\text{Pb}/^{238}\text{U}$  bars correspond to the color of the mapped unit from Figure 2 in the manuscript.

## **Sr and Nd Isotopic Data for the Wichita Igneous Province**

Granites and rhyolites:  $\epsilon_{\text{Nd}} = +1.9$  to  $+4.5$  (Wright et al., 1996; Gilbert and Weaver, 2010).

Basalts:  $\epsilon_{\text{Nd}} = +1.9$  to  $+4.1$ ;  $^{87}\text{Sr}/^{86}\text{Sr}_i = 0.70319$  (Brueseke et al., 2016).

Diabase intrusions:  $\epsilon_{\text{Nd}} = +1.6$  to  $+5.1$ ;  $^{87}\text{Sr}/^{86}\text{Sr}_i = 0.70387$  to  $0.70484$  (Hogan et al., 1995; Gilbert and Weaver, 2010; Lidiak et al., 2014).

Roosevelt Gabbro:  $\epsilon_{\text{Nd}} = +3.3$  to  $+5.1$  (Gilbert and Weaver, 2010).

Glen Mountains Layered Complex:  $\epsilon_{\text{Nd}} = +3.6$  to  $+5.4$ ;  $^{87}\text{Sr}/^{86}\text{Sr}_i = 0.70359$  (Lambert et al., 1988).

## **References**

- Brueseke, M.E., Hobbs, J.M., Bulen, C.L., Mertzman, S.A., Puckett, R.E., Walker, J. D., and Feldman, J., 2016, Cambrian intermediate-mafic magmatism along the Laurentian margin: Evidence for flood basalt volcanism from well cuttings in the Southern Oklahoma Aulacogen (U.S.A.): *Lithos*, v. 260, p. 164–177.
- Gilbert, G.M., and Weaver, B.L., 2010, Petrologic signals related to the rifting process in the Cambrian Southern Oklahoma Aulacogen: *Geological Society of America Abstracts with Programs*, v. 42, no. 5, p. 238.
- Hogan, J.P., Gilbert, M.C., Price, J.D., and Wright, J.E., 1995, Petrogenesis of A-type sheet-granites from an ancient rift, in Brown, M., and Piccoli, P.M., eds., *The Origin of Granites and Related Rocks: Third Hutton Symposium Abstracts: U.S. Geological Survey Circular 1129*, p. 68–69.
- Lambert, D.D., Unruh, D.M., and Gilbert, M.C., 1988, Rb-Sr and Sm-Nd isotopic study of the Glen Mountains Layered Complex: Initiation of rifting within the Southern Oklahoma Aulacogen: *Geology*, v. 16, p. 13–17.
- Lidiak, E.G., Denison, R.E., and Stern, R.J., 2014, Cambrian (?) Mill Creek diabase dike swarm, eastern Arbuckles: A glimpse of Cambrian rifting in the Southern Oklahoma Aulacogen, *in* Suneson, N., ed., *Igneous and Tectonic History of the Southern Oklahoma Aulacogen: Oklahoma Geological Survey Guidebook 38*, p. 105–121.
- Wright, J.E., Hogan, J.P., and Gilbert, M.C., 1996, The Southern Oklahoma Aulacogen: Not just another B.L.I.P.: *American Geophysical Union Transactions*, v. 77, p. F845.